Optically Labeled Dynamic Light Scattering for Ternary Solutions Containing Two Polymer Species

Atsuyuki Ohshima[†] and Takahiro Sato*[,‡]

Department of Macromolecular Science, Osaka University, 1-1 Machikaneyama-cho, Toyonaka, Osaka 560-0043, Japan

Akio Teramoto

Research Organization of Science and Engineering, Ritsumeikan University, and CREST of Japan Science and Technology, Nojihigashi 1-1-1, Kusatsu, Siga 525-8577, Japan

Received May 24, 2000; Revised Manuscript Received August 23, 2000

ABSTRACT: The optically labeled dynamic light scattering (DLS) technique was applied to the ternary system containing two stiff polymers, poly(3-(benzyloxycarbonyl)-*n*-propyl isocyanate) (PBPIC) and poly(*n*-hexyl isocyanate) (PHIC), and toluene being an isorefractive solvent of PHIC, to measure the tracer diffusion coefficient $D_{tr,P}$ of PBPIC (the probe polymer) in semidilute solutions of PHIC (the matrix polymer). $D_{tr,P}$ is appreciably reduced with increasing the matrix polymer concentration. From the comparison with the theory based on the fuzzy cylinder model, it turns out that the intermolecular hydrodynamic interaction between PBPIC and PHIC chains is more important in the reduction of $D_{tr,P}$ than the entanglement interaction. Comparing the present and previous $D_{tr,P}$ data for various ternary solutions including flexible and/or stiff polymers, we have found that the concentration dependence of $D_{tr,P}$ divided by the infinite-dilution value can be scaled by the overlap concentration of the probe polymer in the unperturbed state, irrespective of the chain stiffness, if the overlap concentration of the matrix polymer is much lower than that of the probe polymer.

1. Introduction

The translational motion of polymers in concentrated solutions strongly depends on the polymer concentration, which demonstrates an important role of the interaction among surrounding polymer chains in the polymer mobility.[1−3] To discuss the mobility of polymer chains, the intermolecular interaction of polymers is usually divided into two parts: the short-range entanglement interaction and long-range hydrodynamic interaction. The former interaction is characteristic of linear polymers, and much theoretical effort has been made to understand the entanglement effect on the polymer dynamics.

Effects of the intermolecular interactions on the translational motion of polymer chains have been so far studied by using various experimental techniques, e.g., forced Rayleigh scattering, fluorescence recovery after pattern photobleaching, and optically labeled dynamic light scattering (DLS).[2,3] Those techniques measure the tracer diffusion coefficient $D_{tr,P}$ of a labeled probe (P) polymer chain in a matrix (M) polymer solution as a function of the molecular weights of the P and M polymers as well as the concentration of the M polymer.

The optically labeled DLS technique can be applied to ternary solutions where two chemically different polymer species are dissolved in a solvent, which is an isorefractive solvent of one of the polymer components. For such solutions, light scattering takes place only from the "visible" polymer component, and the DLS experiment can provide us with $D_{tr,P}$ of the visible polymer in the concentrated invisible polymer solution, at infinite dilution of the visible polymer. So far, this technique was applied to several ternary solutions containing two flexible polymers of chemically different kinds.[4−12] The tracer diffusion coefficient of the P chain sharply reduces with increasing the M polymer concentration, which demonstrates that the interaction of the P chain with surrounding M chains makes the translational motion of the P chain remarkably slow.

It is known that the effects of both entanglement and hydrodynamic interactions on the polymer dynamics remarkably depend on the polymer chain stiffness.[1,15,16] Therefore, it may be interesting to compare experimental results of optically labeled DLS for polymer systems with different chain stiffness. Several years ago, Cantor and Pecora[14] measured $D_{tr,P}$ of a flexible polymer, polystyrene, in dilute and semidilute solutions of the stiff polymer, poly(*n*-hexyl isocyanate) (PHIC), by optically labeled DLS. On the other hand, in the present study, we have investigated ternary solutions containing two stiff-chain polymers by the same method. We have chosen poly(3-(benzyloxycarbonyl)-*n*-propyl isocyanate) (PBPIC), recently synthesized by Khatri et al.,[13] as the P polymer, PHIC as the M polymer, and toluene as the solvent. Toluene is an isorefractive solvent of PHIC at 50 °C (for a 488 nm wavelength light), and the persistence lengths q of PBPIC and PHIC in toluene at 50 °C are 12.$_5$ and 32 nm, respectively (see Appendix A), indicating stiff-chain nature of both polymers. Comparing the present and previous data of $D_{tr,P}$, we have found some universal relation with respect to the M polymer concentration dependence of $D_{tr,P}$ in ternary solutions including flexible and/or stiff polymers.

2. Experimental Section

A. Polymer Samples. Samples of poly(3-(benzyloxycarbonyl)-*n*-propyl isocyanate) (PBPIC) were kindly supplied by Prof. M. M. Green at Polytechnic University. Each sample was

[†] Present address: Central Laboratory, Rengo Co., Ltd., 186-1-4, Ohhiraki, Fukushima-ku, Osaka 553-0007, Japan.
[‡] Also at CREST of Japan Science and Technology.

10.1021/ma000915y CCC: $19.00
Published on Web 11/28/2000

Table 1. Molecular Characteristics of PBPIC and PHIC Samples Used in the Optically Labeled DLS Experiment (in Toluene at 50 °C)

sample	$M_w/10^4$	L/nm	N	$A_2/10^{-4}$ [a]	$\langle S^2\rangle^{1/2}$/nm	$[\eta]$/cm^3 g^{-1}	k'
PBPIC (RM-4)	10.5	90.5	3.6	3.0	18.3	79.2	0.41
PHIC (M-2)	13.5[b]	178	2.8			429	0.37

[a] In units of cm^3 mol g^{-2}. [b] Taken from ref 17.

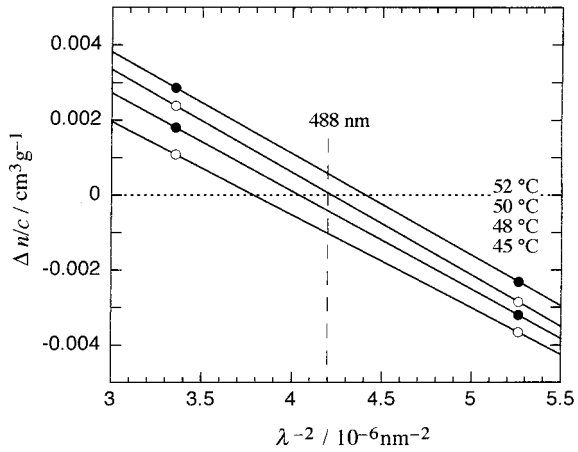

Figure 1. Plots of $\Delta n/c$ against λ^{-2} for toluene solutions of PHIC at different temperatures.

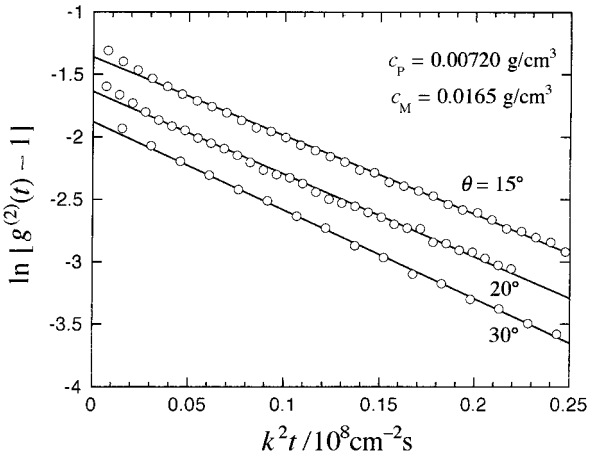

Figure 2. Autocorrelation functions $g^{(2)}(t)$ for a ternary solution of PBPIC, PHIC, and toluene with $c_P = 0.007\,20$ g/cm^3 and $c_M = 0.0165$ g/cm^3 at 50 °C.

divided into several fractions by repeating fractional precipitation with benzene as the solvent and methanol as the precipitant. A middle fraction, named RM-4, was chosen for the optically labeled DLS experiment, and several middle fractions were used to determine the wormlike chain parameters in 50 °C toluene (cf. Appendix A). A fractionated PHIC sample was chosen as the matrix polymer in optically labeled DLS, which was used in a previous study[17] (sample M-2).

The weight-average molecular weight M_w, the radius of gyration $\langle S^2\rangle^{1/2}$, the second virial coefficient A_2, the intrinsic viscosity $[\eta]$, and the Huggins coefficient k' of the PBPIC sample RM-4 were determined in toluene at 50 °C by static light scattering and viscometry. The procedure of static light scattering and viscometry was described elsewhere.[18] For the PHIC sample M-2, M_w was previously determined in dichloromethane at 20 °C by static light scattering,[17] and $[\eta]$ and k' in toluene at 50 °C were estimated in this study. Results for the two samples are listed in Table 1.

The wormlike chain parameters of PBPIC and PHIC in toluene at 50 °C are estimated in Appendix A. Using those parameters, the contour lengths L and the number of Kuhn's statistical segments N for the two samples RM-4 and M-2 were calculated from M_w, which are also listed in Table 1.

B. Differential Refractometry. A differential refractometer of the modified Schulz-Cantow type was used to measure excess refractive indices Δn of toluene solutions of PHIC at the light wavelength $\lambda = 436$ and 546 nm at several temperatures. Since the refractive index increment $\partial n/\partial c$ was very small, the measurements were extended up to a PHIC concentration c as high as 0.07 g/cm^3. Figure 1 plots the results of $\Delta n/c$ at different temperatures against λ^{-2}. This plot shows $\partial n/\partial c$ of PHIC in toluene at $\lambda = 488$ nm to become zero at 50 °C.

Excess refractive indices Δn of toluene solutions of PBPIC at $\lambda = 436$ and 546 nm were also measured at 50 °C by the same refractometer, and from the interpolation of the results, $\partial n/\partial c$ of PBPIC in 50 °C toluene at $\lambda = 488$ nm was estimated to be 0.0710 cm^3/g. Thus, PBPIC possesses the ability of light scattering in toluene solution at 50 °C.

C. Dynamic Light Scattering. Toluene solutions of the PBPIC and PHIC samples with concentrations of 0.015 g/cm^3 or less were separately prepared and filtrated through Millipore filters with a 0.2 μm pore size. Then the PHIC solutions were gently heated (below the boiling temperature) to evaporate the solvent slowly, until they reach to given concentrations. These concentrated PHIC solutions were mixed with the PBPIC solution in appropriate ratios to obtain test solutions of optically labeled DLS measurements. Before the measurements, the test solutions were centrifuged at ca. 12 000g.

The normalized autocorrelation function $g^{(2)}(t)$ of scattered light intensity for each test solution was measured at 50 °C by a light scattering goniometer (JASCO, Lsp-20) equipped with a photon correlator (Unisoku, DP-200) with an argon ion laser (NEC, GLG3110) emitting vertically polarized light of 488 nm wavelength as light source.

3. Results

Figure 2 shows autocorrelation functions $g^{(2)}(t)$ for a ternary solution of PBPIC, PHIC, and toluene measured at 50 °C and at three different scattering angles θ. The mass concentrations of the probe (P) polymer (PBPIC) c_P and the matrix (M) polymer (PHIC) c_M of the solution were 0.00720 and 0.0165 g/cm^3, respectively. In the abscissa, the delay time t is multiplied by the square of the scattering vector k^2. Except at very short t, data points for each θ follow a straight line, whose slope becomes slightly steeper with increasing θ or k^2. The deviations of the points at short t may reflect fast internal motions of PBPIC or PHIC. It is verified theoretically that the motion of the invisible M polymer chains can affect $g^{(2)}(t)$ through the cross-correlation between the P and M polymers.[12] Previously, several workers reported weak nonexponential decays of $g^{(2)}(t)$ in optically labeled DLS experiments for various ternary polymer solutions.[5,6,8,14]

From the slope of the line drawn with neglecting the short t data points, we estimated the decay rate Γ as a function of k or θ. Figure 3 shows the k^2 dependence of Γ divided by k^2, where we collect results of Γ/k^2 for ternary solutions with constant total polymer concentration c ($\equiv c_P + c_M$) = 0.0237 g/cm^3 and different c_P. For all solutions displayed, Γ/k^2 is a weakly increasing function of k^2. This k^2 dependence may be related also to the effect of fast internal motions of the P and M polymer motions.

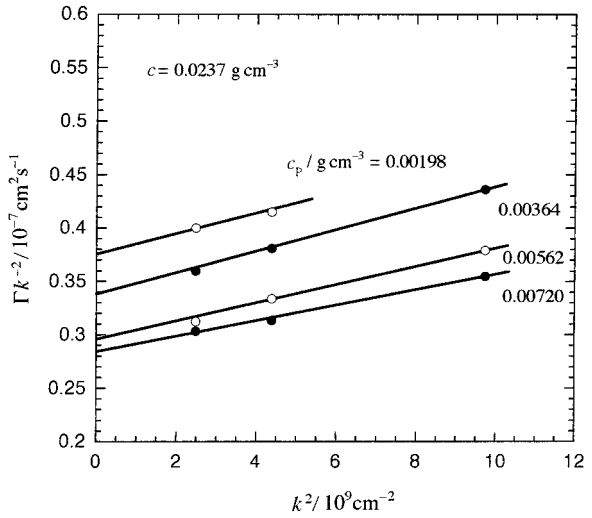

Figure 3. Dependence of Γ/k^2 on k^2 for ternary solutions of PBPIC/PHIC/toluene with the total polymer concentration c ($\equiv c_P + c_M$) = 0.0237 g/cm^3 and different c_P.

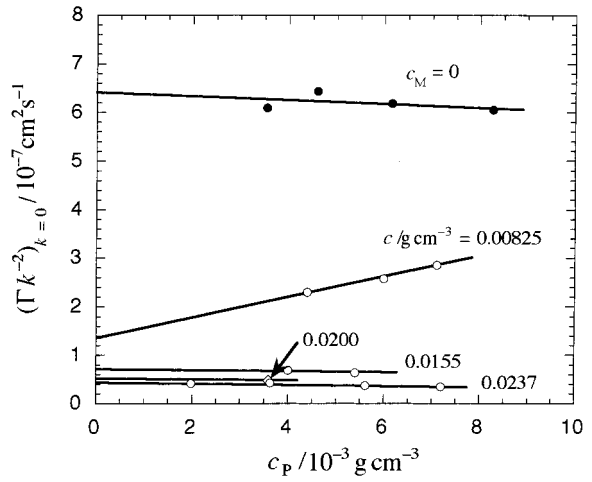

Figure 4. Plots of $(\Gamma/k^2)_{k=0}$ vs c_P for ternary solutions of PBPIC/PHIC/toluene under the constant total polymer concentration c.

Values of Γ/k^2 at $k^2 = 0$ [$(\Gamma/k^2)_{k=0}$], obtained by the extrapolation, are plotted against c_P under the constant total polymer concentration c in Figure 4 (unfilled circles and a diamond). Since the total polymer concentration is fixed, the entanglement and hydrodynamic interactions in the ternary solutions may not be so much altered when c_P is changed. However, the effect of the cross-correlation between PBPIC and PHIC on $g^{(2)}(t)$ or Γ must be modified during the change of c_P or the relative composition of the P and M polymers.[12] This change in the composition is most drastic at the lowest c, and a strong c_P dependence of $(\Gamma/k^2)_{k=0}$ at c = 0.008 25 g/cm^3 may come from the change in the cross-correlation effect. When c is increased, the c_P dependence of $(\Gamma/k^2)_{k=0}$ becomes weak and also reverses from negative to positive.[19] We have estimated the tracer diffusion coefficient $D_{tr,P}$ of the P polymer in the solution of the M polymer with the concentration $c_M = c$, by extrapolating $(\Gamma/k^2)_{k=0}$ to $c_P = 0$. Although there is only one data point for c = 0.0200 g/cm^3 (the diamond in Figure 4), we have extrapolated this result to $c_P = 0$, using a line with the same slope as the fitting line for c = 0.0237 g/cm^3. In Figure 4, filled circles indicate the c_p dependence of $(\Gamma/k^2)_{k=0}$ for toluene solutions of PBPIC without containing PHIC. We have estimated the translational diffusion coefficient $D_{0,P}$ of PBPIC in pure toluene by extrapolation to $c_P = 0$.

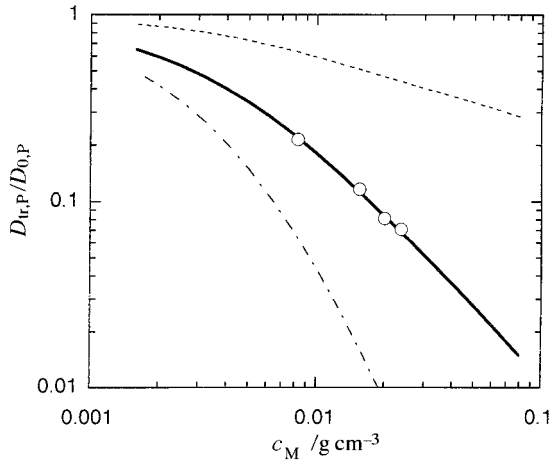

Figure 5. Matrix-polymer concentration c_M dependence of $D_{tr,P}/D_{0,P}$ for ternary solutions of PBPIC/PHIC/toluene at 50 °C: circles, experimental data; solid and dotted curves, theoretical values calculated by eq B.9 with $k'_{HI,PM}$ = 0.53 and 0, respectively; dash−dotted curve, values calculated by eq 2.

Figure 5 shows the c_M dependence of the tracer diffusion coefficient $D_{tr,P}$ divided by $D_{0,P}$ for PBPIC in toluene solutions of PHIC at 50 °C by circles. The data points almost follow a line with the slope of −1.1 within the c_M range examined. This result indicates that the translational motion of the PBPIC chain is effectively hindered by surrounding PHIC chains in toluene solution through entanglement and hydrodynamic interactions. In the following section, we will estimate the contribution of the entanglement interaction to the slowing down of the PBPIC chain motion using a theory based on the fuzzy cylinder model and compare the theoretical result with the experimental $D_{tr,P}/D_{0,P}$ to assess the importance of the hydrodynamic interaction. Furthermore, the c_M dependence of $D_{tr,P}/D_{0,P}$ for PBPIC in PHIC solutions will be compared with corresponding experimental results for other ternary solutions containing two flexible polymer components and flexible- and stiff-polymer components reported so far.

4. Discussion

A. Comparison with the Theory of the Fuzzy Cylinder Model. Local conformational changes of a semiflexible chain are expected to be much faster than the center-of-mass translation of the chain. The changes make segments of the chain distribute symmetrically around the chain end-to-end axis, and thus the polymer chain may be modeled by a smoothed-density cylinder (the fuzzy cylinder).[16] As a result, global motions of entangled polymer chains can be represented by motions of colliding fuzzy cylinders. In a previous paper,[17] we have demonstrated that this fuzzy cylinder model is suitable to describe the translational motion of PHIC in semidilute solution, by comparing experimental results of the mutual diffusion coefficient D_m with the theory based on this model.

The geometry of the fuzzy cylinder is specified by the effective length L_e and effective diameter d_e, which are calculated by[16]

$$L_e = \langle R^2 \rangle^{1/2}, \quad d_e = \left[\left\langle H\left(\frac{1}{2}L\right)^2 \right\rangle + d^2 \right]^{1/2} \qquad (1)$$

Table 2. Molecular Characteristics of Polymer Samples Used in Optically Labeled DLS Experiments Reported So Far

symbol[a]	P polymer	M polymer	$M_P/10^4$	$M_M/10^4$	$[\eta]_{0,P}$/cm^{-3} g	$[\eta]_{0,M}$ cm^{-3} g	ϕ^*_P	ϕ^*_M	ref
●	PBPIC	PHIC	10.5	13.5	79.2	429	0.0124	0.0023	present study
▲	PS	PHIC	39	15	55[b]	2.47	0.0169	0.004	14
▼			39	5.27	55[b]	0.88	0.0169	0.0113	14
◆			39	4.5	55[b]	0.74	0.0169	0.0133	14
⊡	PS	PVME	105	130	90.2[b]	449[c]	0.0103	0.00219[c]	11
⧄			42.2	130	57.2[b]	449[c]	0.0162	0.00219[c]	11
□			17.9	130	37.2[b]	449[c]	0.025	0.00219[c]	11
□			6.5	130	22.4[b]	449[c]	0.0414	0.00219[c]	11
○	PS	PMMA	842	405	255[b]	105[d]	0.00364	0.00811	10
⊙			842	193	255[b]	72.8[d]	0.00364	0.0117	10
◇			42	405	57[b]	105[d]	0.0162	0.00811	10
△	PMMA	PS	34.2	842	30.6[d]	255[b]	0.0279	0.00364	8
▽			34.2	77.5	30.6[d]	77.5[b]	0.0279	0.012	8
×			34.2	18.6	30.6[d]	37.9[b]	0.0279	0.0244	8
+			34.2	4.39	30.6[d]	18.4[b]	0.0279	0.0503	8

[a] Symbols used in Figures 6 and 7. [b] Values in cyclohexane at 34.5 °C calculated by $[\eta]_0 = 0.088M^{0.5}$ cm^3/g.[34] [c] Value in 30 °C *o*-fluorotoluene (in the non-θ state). [d] Values in acetonitrile at 44 °C calculated by $[\eta]_0 = 0.0524M^{0.5}$ cm^3/g.[35]

Table 3. Wormlike Cylinder Parameters of PBPIC and PHIC in Different Solvents

solvent	temp/°C	q/nm	M_L/nm^{-1}	d/nm
(1) PBPIC				
toluene	50	$12._5 \pm 1$	1160 ± 30	1.6[a]
	25	$15._5 \pm 1._5$	1150 ± 50	1.6[a]
dichloromethane	20	22 ± 2	1130 ± 50	1.6[a]
(2) PHIC				
toluene	50	32 ± 5	760 ± 40	1.6[a]
	25[b]	37	740	1.6
dichloromethane	20[b]	21	740	1.6

[a] Assumed value. [b] Taken from ref 25.

where $\langle R^2 \rangle$ and $\langle H(^1/_2L)^2 \rangle$ are the mean-square end-to-end distance and the mean-square distance of the chain midpoint from the end-to-end axis, respectively, and d is the diameter of the polymer chain. By using the wormlike chain model, $\langle R^2 \rangle$ and $\langle H(^1/_2L)^2 \rangle$ are calculated from the persistence length q, the molar mass per unit contour length M_L, and the polymer molecular weight.[16] As described in Appendix A, the wormlike cylinder parameters, q, M_L, and d, for PBPIC and PHIC in toluene at 50 °C were determined from the intrinsic viscosity data. The results are listed in Table 3. Using the results (the mean values of q and M_L) along with the sample molecular weights, L_e and d_e are estimated to be 44 and 15 nm for the PBPIC sample RM-4 and to be 97 and 31 nm for the PHIC sample M-2, respectively. Since the intramolecular excluded-volume effect and its screening in concentrated solutions are not expected for either stiff polymer, conformations of the two polymers are assumed to be independent of the PHIC concentration in what follows.

The theory used previously[17] can be easily extended to ternary systems consisting of two stiff polymers and a solvent. The theoretical expression of the tracer diffusion coefficient $D_{tr,P}$ of the P chain in M polymer solutions is given in Appendix B. Equation B.9 contains the only unknown parameter $k'_{HI,PM}$, the strength of the hydrodynamic interaction exerted on the P polymer by the M polymer. With this parameter taken to be zero, eq B.9 is used to estimate the contribution of the entanglement effect to the slowing down of the translational motion of the P chain in M polymer solutions. In Figure 5, the dotted curve shows the theoretical values of $D_{tr,P}/D_{0,P}$ calculated by eq B.9 with $k'_{HI,PM} = 0$. This theoretical result is much more weakly dependent on c_M than the experimental results, indicating that the entanglement effect on the P chain diffusivity by surrounding M chains is not predominant in the ternary system of PBPIC (the P polymer), PHIC (the M polymer), and toluene.

When the value of $k'_{HI,PM}$ is increased, the theoretical $D_{tr,P}/D_{0,P}$ exhibits stronger c_M dependence, and at $k'_{HI,PM} = 0.53$ the theoretical curve fits most satisfactorily to the experimental data points, as shown by the solid curve in Figure 5. A previous paper[20] mentioned that the strength parameter k'_{HI} of the intermolecular hydrodynamic interaction can be estimated from experimental Huggins coefficient k' for binary polymer solutions. In the same procedure, we can estimate the sum of $k'_{HI,PM}$ and $k'_{HI,MP}$ from experimental k' of dilute ternary solutions containing the P and M polymers, where $k'_{HI,MP}$ is the strength of the hydrodynamic interaction exerted on the M polymer by the P polymer. We have measured k' for toluene solutions of the PBPIC (RM-4) and PHIC (M-2) samples at 50 °C as a function of the relative composition of the two samples and analyzed the results to obtain $k'_{HI,PM} + k'_{HI,MP} = 0.68$. Both $k'_{HI,PM}$ and $k'_{HI,MP}$ must be positive from their physical meanings, so that each of them must be smaller than their sum, 0.68. Therefore, it is compatible with the value of 0.53 for $k'_{HI,PM}$ used in Figure 5 (the solid curve), which could give a positive value of $k'_{HI,MP}$, although the two coefficients cannot be separately estimated from k' data alone.

According to the previous theory for binary polymer solutions,[17,20] we can estimate the strengths of the hydrodynamic interaction in binary toluene solutions of the PBPIC (RM-4) and PHIC (M-2) samples from the experimental k' listed in the last column of Table 1; $k'_{HI,PP} = 0.15$ for the PBPIC sample and $k'_{HI,MM} = 0.021$ for the PHIC sample. Those values for the stiff polymers are considerably smaller than k'_{HI} for binary solutions of flexible polymers ($\approx$0.4−0.6).[20] On the other hand, $k'_{HI,PM}$ obtained above is comparable to k'_{HI} for binary flexible polymer solutions and larger than $k'_{HI,PP}$ and $k'_{HI,MM}$, indicating importance of the cross hydrodynamic interaction in ternary solutions containing two stiff polymers.

If the M polymer solution is regarded as a continuous medium with the zero-shear viscosity η_0, $D_{tr,P}/D_{0,P}$ may be calculated by using the Einstein−Stokes relation simply as

$$D_{tr,P}/D_{0,P} = \eta^{(S)}/\eta_0 \qquad (2)$$

where $\eta^{(S)}$ is the solvent viscosity. The dash−dotted curve in Figure 5 indicates the result calculated by this

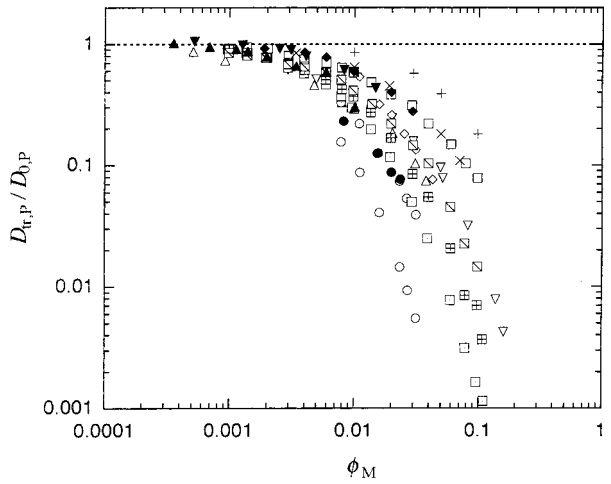

Figure 6. Comparison of $D_{tr,P}/D_{0,P}$ for ternary solutions of PBPIC/PHIC/toluene, polystyrene (PS)/PHIC/1,1,2,2-tetrachloroethane,[14] PS/poly(vinyl methyl ether) (PVME)/*o*-fluorotoluene,[11] PS/poly(methyl methacrylate) (PMMA)/benzene,[10] and PMMA/PS/thiophenol,[8] obtained by the optically labeled DLS experiment so far. Symbols are explained in Table 2.

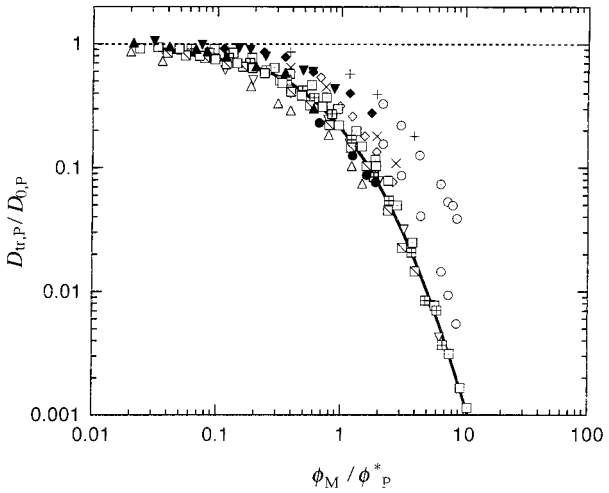

Figure 7. Plots of $D_{tr,P}/D_{0,P}$ against ϕ_M/ϕ^*_P for various ternary solutions. Symbols are the same as those used in Figure 6 (cf. Table 2), and the solid curve represents an experimental master curve.

equation, where η_0 for toluene solutions of PHIC at 50 °C was estimated by the fuzzy cylinder model theory, which was demonstrated to accurately predict η_0 of PHIC solutions in various solvent conditions.[17] This theoretical curve exhibits much stronger c_M dependence than the experimental results. Thus, we can say that the M polymer solution should not be regarded as a continuous medium in the argument of the translational diffusivity of the P chain.

B. Comparison with Optically Labeled DLS Results for Other Ternary Polymer Solutions. So far, the optically labeled DLS technique has been applied to several ternary solutions containing a pair of flexible polymers[4−12] and also flexible and stiff polymers,[14] to investigate the hindrance of the translational diffusivity of a P chain by surrounding M polymer chains. Figure 6 collects experimental results of the optically labeled DLS reported so far for various ternary polymer solutions. Here $D_{tr,P}/D_{0,P}$ is plotted against the volume fraction ϕ_M of the M polymer, which was calculated by the equation $\phi_M = \bar{v}_M c_M$ with the partial specific volume $\bar{v}_M$ of the M polymer, and each system plotted in the figure is specified in Table 2. It is seen that the data points for different combinations of P and M follow different curves, indicating that the hindering effect on $D_{tr,P}$ depends on molecular weights of the P (M_P) and M (M_M) chains in each ternary polymer solution.

In Figure 7, $D_{tr,P}/D_{0,P}$ is plotted against ϕ_M divided by the overlap volume fraction ϕ^*_P of the P polymer, which was calculated by $\phi^*_P = \bar{v}_P/[\eta]_{0,P}$ with $[\eta]_{0,P}$ the intrinsic viscosity of the P chain in the unperturbed state. The data points fulfilling the condition $\phi^*_P \gg \phi^*_M$ ($= \bar{v}_M/[\eta]_{0,M}$), namely those except for symbols, ▼, ◆, ○, ⊙, ×, and +, almost follow a master curve (the solid curve), irrespective of the kinds of P and M polymers. The data points (filled circles) for the PBPIC/PHIC/toluene system obtained in this study also follow the master curve. This universal plot was originally proposed by Wheeler et al.[11] The M chain starts overlapping at $\phi_M = \phi^*_M$, but the hindrance of the P chain translation is not appreciable at this concentration of the M polymer. Figure 7 indicates that the hindrance becomes effective at $\phi_M = \phi^*_P$ ($\gg\phi^*_M$), where the volume fraction of the M polymer in bulk solution becomes identical with the local volume fraction inside one P chain in the unperturbed state, irrespective the polymer chain stiffness. The intramolecular excluded-volume effect for the P chain may be screened out in the M polymer solution at $\phi_M = \phi^*_P$. (Stiff polymers with sufficiently small Kuhn segment number N are free from the excluded-volume effect even in dilute solution.[34])

It is known that the overlap concentration (or the local concentration inside the single chain) of stiff polymers is very low in comparison with that of flexible polymers due to their extended conformations. As seen from the master curve in Figure 7, this overlap concentration is the key parameter in the hindrance of the translational motion of the P polymer chain, so that we can say that the hindrance is more effective for stiff polymers than for flexible polymers.

5. Concluding Remarks

We have compared the dependence of the P polymer tracer diffusion coefficient $D_{tr,P}$ on the M polymer concentration ϕ_M for various ternary polymer solutions obtained by the optically labeled DLS and found the universal relation of $D_{tr,P}/D_{0,P}$ to ϕ_M/ϕ^*_P under the condition $\phi^*_P \gg \phi^*_M$, irrespective of chain stiffness of both P and M polymers (cf. Figure 7). As mentioned in section 4A, the cross hydrodynamic interaction between P and M polymers plays an important role in the ϕ_M dependence of $D_{tr,P}$. However, no theoretical evaluations of the cross hydrodynamic interaction has been made for ternary polymer solutions so far. Thus, the universal relation shown in Figure 7 has not been theoretically verified yet.

For binary polymer solutions, where the M polymer is identical with the P polymer, the universal plot of $D_{tr,P}/D_{0,P}$ vs ϕ_M/ϕ^*_P corresponds to the plot of D_s/D_0 against $c[\eta]$. Here, D_s and D_0 are the self-diffusion coefficient and the diffusion coefficient at infinite dilution, respectively. Since the binary solutions do not fulfill the condition $\phi^*_P \gg \phi^*_M$, this plot for binary polymer solutions may not be universal. In a previous study, Ohshima et al.[17] measured the mutual diffusion coefficient D_m for dichloromethane solutions of four PHIC samples with different molecular weights M. The self-diffusion coefficient for this system may be calcu-

lated by the equation $D_s = D_m/[(M/RT)(\partial\Pi/\partial c)(1 - \bar{v}c)$, where Π is the osmotic pressure, RT is the gas constant multiplied by the absolute temperature, and $\bar{v}$ is the partial specific volume of the polymer, and the results of D_s are shown in Figure 11 of ref 17. Although not shown here, the plot of D_s/D_0 against $c[\eta]$ for the four PHIC samples did not follow a single master curve. This demonstrates the necessity for the condition of $\phi^*_P \gg \phi^*_M$ to the above universal relation.

Acknowledgment. We are grateful to Professor Mark M. Green at the Polytechnic University, who kindly provided us with poly(3-(benzyloxycarbonyl)-*n*-propyl isocyanate) samples. A.T. thanks Yamashita Construction Design Inc. for the Chair-Professorship at Ritsumeikan University. This work was supported by a Grant-in-Aid for Scientific Research (No. 07651110) from the Ministry of Education, Science, Sports, and Culture of Japan.

Appendix A. Wormlike Chain Parameters of Poly(3-(benzyloxycarbonyl)-*n*-propyl isocyanate)

Recently, Khatri et al.[13] synthesized poly(3-(benzyloxycarbonyl)-*n*-propyl isocyanate) (PBPIC) and demonstrated that this polymer is miscible with a flexible random copolymer of vinylphenol (9%) and styrene (91%) probably through the hydrogen bonding between the two polymer components. This appendix analyzes the chain stiffness of PBPIC in solution in terms of the wormlike chain model. The wormlike chain parameters are necessary to compare optically labeled DLS results with the fuzzy cylinder model theory.

The wormlike chain parameters can be determined from the molecular weight dependence of the intrinsic viscosity $[\eta]$. The weight-average molecular weight M_w and $[\eta]$ were measured for six fractionated PBPIC samples by static light scattering and viscometry, respectively. The light scattering experiment was made for dichloromethane (DCM) solution at 20 °C, while viscometry was made for DCM solutions at 20 °C and also for toluene solutions at 50 and 25 °C. The refractive index increment $\partial n/\partial c$ of PBPIC in DCM at 20 °C was measured to be 0.132 cm^3/g at $\lambda = 436$ nm. Detailed experimental procedures are described elsewhere.[21]

Figure 8 shows the molecular weight dependence of $[\eta]$ for PBPIC obtained in 50 °C toluene and 20 °C DCM. The viscosity exponents in a low-M_w region ($1 < M_w/10^5 < 3$) are 0.93 and 1.0 for toluene and DCM solutions, respectively, definitely indicating the stiff-chain nature of PBPIC in both solvents.[24]

We have analyzed the $[\eta]$ data using the wormlike cylinder model, which characterizes the polymer chain in terms of the persistence length q, the contour length L, and cylinder diameter d. The contour length is related to the molecular weight M by the shift factor (i.e., the molar mass per unit contour length) M_L by $L = M/M_L$. According to the Yamakawa−Fujii−Yoshizaki (YFY) theory,[22−24] $[\eta]$ for the wormlike cylinder model can be calculated as a function of M, provided q, M_L, and d are given. Since $[\eta]$ is insensitive to the value of d, we have assumed the value of d for PBPIC to be the same as that of PHIC (=1.6 nm)[25] and determined q and M_L by fitting experimental data to theoretical $[\eta]$ calculated by the YFY theory. In Figure 8, solid curves show examples of the fitting where theoretical values of $[\eta]$ were calculated by the YFY theory with $q = 12._5$ nm and $M_L = 1160$ nm^{-1} in 50 °C toluene and with $q = 22$ nm and $M_L = 1130$ nm^{-1} in 20 °C DCM. Similar fitting was obtained also using different pairs of q and M_L. Table 3 summarizes the ranges of q and M_L which provide good fits to $[\eta]$ data of PBPIC in 50 °C toluene and 20 °C DCM.

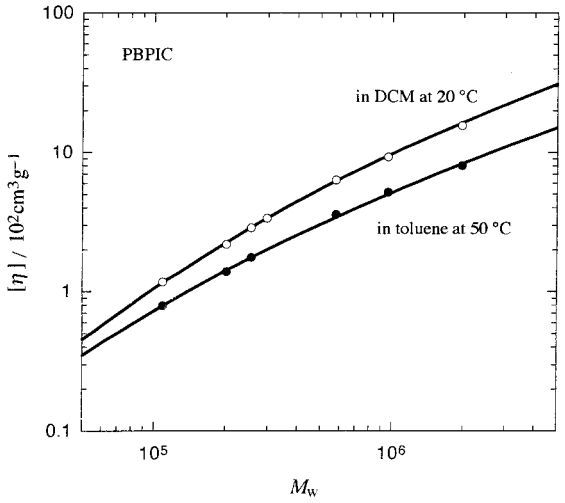

Figure 8. Molecular weight dependence of the intrinsic viscosity $[\eta]$ for PBPIC in toluene at 50 °C (●) and in DCM at 20 °C (○); curves, theoretical values calculated by the Yamakawa−Fujii−Yoshizaki theory.[22−24]

In the same method, we have determined q and M_L for PBPIC in toluene at 25 °C and for PHIC in toluene at 50 °C. Table 3 also lists those results as well as the previous results[25] for PHIC in 25 °C toluene and 20 °C DCM. For PHIC, the value of q is larger in toluene than that in more polar solvent, DCM. However, this order of q is reversed for PBPIC. In DCM, the q of PBPIC is practically equal to that of PHIC, but in toluene it is much smaller than that of PHIC. It is noted that the order of the second virial coefficient A_2 for PBPIC in toluene and DCM is also reversed in comparison with that for PHIC;[21,26] A_2 of the PBPIC sample RM-4 is 5.5×10^{-4} in 20 °C DCM and 3.0×10^{-4} in 50 °C toluene. The polar side chain of PBPIC influences both the chain stiffness and intermolecular interaction of polyisocyanate chains.

Appendix B. Formulation of the Tracer Diffusion Coefficient Based on the Fuzzy Cylinder Model

Previously, Sato et al.[27] formulated the rotational diffusion coefficient of a stiff polymer in multicomponent stiff-polymer solutions by the mean-field Green function method based on the fuzzy cylinder model. The same procedure can be applied to formulate the transverse diffusion coefficient $D_{\perp,P}$ of the probe (P) stiff polymer in solutions of the matrix (M) stiff polymer. Here, $D_{\perp,P}$ means the self-diffusion coefficient in the direction perpendicular to the end-to-end (or the fuzzy cylinder) axis of the P chain. For simplicity, we here consider only the case that the effective length $L_{e,P}$ of the fuzzy cylinder for the P chain is shorter than the effective length $L_{e,M}$ for the M chain and also $c_P = 0$. The optically labeled DLS experiment performed in the present study corresponds to this case ($L_{e,P} = 44$ nm; $L_{e,M} = 97$ nm).

Under the condition mentioned above, $D_{\perp,P}$ is written as[16,20,27]

$$\frac{D_{\perp,\mathrm{P}}}{\hat{D}_{\perp 0,\mathrm{P}}} = \left\{1 + \frac{1}{\sqrt{\beta_\perp}} L_{\mathrm{e,M}}^2 L_{\mathrm{e,P}} f_\perp(x,y) c'_{\mathrm{M}} \left(\frac{2D_{\perp 0,\mathrm{P}}}{D_{\parallel 0,\mathrm{P}}}\right)^{1/2} \left(\frac{\hat{D}_{\parallel 0,\mathrm{P}}}{D_{\parallel,\mathrm{P}}}\right)^{1/2}\right\} \quad \text{(B.1)}$$

where $\beta_\perp$ is a numerical constant, c'_{M} is the number concentration of M chains, $D_{\parallel,\mathrm{P}}$ is the longitudinal diffusion coefficient of the P chain in the direction parallel to the end-to-end axis, $D_{\perp 0,\mathrm{P}}$ and $D_{\parallel 0,\mathrm{P}}$ are $D_{\perp,\mathrm{P}}$ and $D_{\parallel,\mathrm{P}}$ at $c'_{\mathrm{M}} = 0$, respectively, $\hat{D}_{\perp 0,\mathrm{P}}$ and $\hat{D}_{\parallel 0,\mathrm{P}}$ are $D_{\perp,\mathrm{P}}$ and $D_{\parallel,\mathrm{P}}$ at switching off the entanglement effect, respectively, and $f_\perp(x,y)$ is the function defined by

$$f_\perp(x,y) = \frac{1}{3}(1 + 2x + C_\perp y)\left[\frac{\frac{\pi}{2}x^2 + (J-1)x}{\frac{\pi}{2} - 1} + C_\perp y\right] \quad \text{(B.2)}$$

with

$$x \equiv L_{\mathrm{e,P}}/L_{\mathrm{e,M}}, \quad y \equiv d_{\mathrm{e,M}}/L_{\mathrm{e,M}}, \quad J \equiv \sqrt{1-x^2}\,\ln[(1+\sqrt{1-x^2})/x] \quad \text{(B.3)}$$

The function $f_\perp$ corresponds to the f_{r} function in the previous paper,[27] which is a finite-thickness correction factor for the hindering cylinder. The parameter $C_\perp$ in eq B.2 represents the effectiveness of the hindrance release by the segment fluctuation inside the fuzzy cylinder and is empirically expressed as a function the Kuhn segment number N_{M} of the M chain as[16]

$$C_\perp = \frac{1}{2}\left(\tanh\frac{N_{\mathrm{M}} - N^*}{\Delta} + 1\right) \quad \text{(B.4)}$$

with the two numerical constants N^* and Δ, which were previously determined as $N^* = \Delta = 4$ for PHIC solutions.[17] The another constant $\beta_\perp$ in eq B.1 was determined by Teraoka[28] to be 560 from a stochastic geometric argument by use of the cage model for rodlike polymers.

The longitudinal diffusion coefficient $D_{\parallel,\mathrm{P}}$ of the P chain in the M polymer solution can be calculated by the hole theory, used in previous studies.[16,29] In the present optically labeled DLS experiment, we have chosen the P and M polymer samples in the condition that the effective diameter $d_{\mathrm{e,P}}$ of the fuzzy cylinder for the P chain (=15 nm) is smaller than the effective diameter $d_{\mathrm{e,M}}$ of the M chain (=31 nm). In this case, we have[29]

$$D_{\parallel,\mathrm{P}}/\hat{D}_{\parallel 0,\mathrm{P}} = \exp(-V_{\mathrm{ex,M}}^{*(\mathrm{P})} c'_{\mathrm{M}}) \quad \text{(B.5)}$$

where

$$V_{\mathrm{ex,M}}^{*(\mathrm{P})} = F(\lambda^* L_{\mathrm{e,P}}, \lambda^* d_{\mathrm{e,P}}; L_{\mathrm{M}}, d_{\mathrm{M}}) \quad \text{(B.6)}$$

with the function F defined by

$$F(L_1,d_1;L_2,d_2) = \frac{\pi}{4}\Big[L_1L_2(d_1+d_2) + (L_1{d_1}^2 + L_2{d_2}^2) + \frac{1}{2}({L_1}^2 d_1 + {L_2}^2 d_2) + \frac{\pi}{2}(L_1+L_2)d_1d_2 + \frac{\pi}{4}(d_1+d_2)d_1d_2\Big] \quad \text{(B.7)}$$

and the contour length L_{M}, the diameter d_{M} of the M chain, and the similarity ratio λ^* between the critical hole and the fuzzy cylinder of the P chain. Previously, λ^* was estimated to be 0.03 in binary solutions of PHIC, irrespective of the kind of solvent.[17] Furthermore, λ^* has been recently demonstrated to be close to 0.03 also for a cellulose derivative[30] whose q is similar to PBPIC in 50 °C toluene.[31] Thus, we assume the same value for λ^* in the ternary system of PBPIC, PHIC, and toluene.

Finally, we consider the intermolecular hydrodynamic interaction in multicomponent polymer solutions. The hydrodynamic interaction modifies the diffusion coefficients $\hat{D}_{\perp 0,\mathrm{P}}$ and $\hat{D}_{\parallel 0,\mathrm{P}}$ at switching off the entanglement effect. As in the previous paper,[17] the polymer concentration dependences of $\hat{D}_{\perp 0,\mathrm{P}}$ and $\hat{D}_{\parallel 0,\mathrm{P}}$ are assumed to be identical and considered up to the linear order of the concentration. At infinite dilution of the P polymer, those diffusion coefficients are written as

$$\frac{D_{\parallel 0,\mathrm{P}}}{\hat{D}_{\parallel 0,\mathrm{P}}} = \frac{D_{\perp 0,\mathrm{P}}}{\hat{D}_{\perp 0,\mathrm{P}}} = 1 + k'_{\mathrm{HI,PM}}[\eta]_{\mathrm{M}} c_{\mathrm{M}} \quad \text{(B.8)}$$

where $k'_{\mathrm{HI,PM}}$ is the strength of the hydrodynamic interaction exerted on the P polymer by the M polymer, and $[\eta]_{\mathrm{M}}$ is the intrinsic viscosity of the M polymer.

The tracer diffusion coefficient $D_{\mathrm{tr,P}}$ of the infinitely diluted P chain in M polymer solutions is calculated by[17]

$$D_{\mathrm{tr,P}} = \frac{1}{3}(D_{\parallel,\mathrm{P}} + 2D_{\perp,\mathrm{P}}) = D_{0,\mathrm{P}}\frac{(D_{\parallel,\mathrm{P}}/\hat{D}_{\parallel 0,\mathrm{P}}) + 2(D_{\perp 0,\mathrm{P}}/D_{\parallel 0,\mathrm{P}})(D_{\perp,\mathrm{P}}/\hat{D}_{\perp 0,\mathrm{P}})}{(1 + 2D_{\perp 0,\mathrm{P}}/D_{\parallel 0,\mathrm{P}})(1 + k'_{\mathrm{HI,PM}}[\eta]_{\mathrm{M}} c_{\mathrm{M}})} \quad \text{(B.9)}$$

where $D_{0,\mathrm{P}}$ is the translational diffusion coefficient of the P chain at $c_{\mathrm{P}} = c_{\mathrm{M}} = 0$. The ratio $D_{\perp 0,\mathrm{P}}/D_{\parallel 0,\mathrm{P}}$ is a hydrodynamic parameter at infinite dilution, being calculated by the hydrodynamic theory.[16] Therefore, if the only unknown parameter $k'_{\mathrm{HI,PM}}$ is given, we can calculate $D_{\mathrm{tr,P}}/D_{0,\mathrm{P}}$ as a function of c_{M}.

References and Notes

(1) Doi, M.; Edwards, S. F. *The Theory of Polymer Dynamics*; Clarendon Press: Oxford, 1986.
(2) Fujita, H. *Polymer Solutions*; Elsevier: Amsterdam, 1990; Vol. 9.
(3) Tirrell, M. *Rubber Chem. Technol.* **1984**, *57*, 52.
(4) Lodge, T. P. *Macromolecules* **1983**, *16*, 1393.
(5) Martin, J. E. *Macromolecules* **1984**, *17*, 1279.
(6) Nemoto, N.; Inoue, T.; Tsunashima, Y.; Kurata, M. *Bull. Inst. Chem. Res., Kyoto Univ.* **1984**, *62*, 177.
(7) Hanley, B.; Tirrell, M.; Lodge, T. P. *Polym. Bull.* **1985**, *14*, 137.
(8) Nemoto, N.; Inoue, T.; Makita, Y.; Tsunashima, Y.; Kurata, M. *Macromolecules* **1985**, *18*, 2516.
(9) Numasawa, N.; Hamada, T.; Nose, T. *J. Polym. Sci., Polym. Phys. Ed.* **1986**, *24*, 19.
(10) Numasawa, N.; Kuwamoto, K.; Nose, T. *Macromolecules* **1986**, *19*, 2593.
(11) Wheeler, L. M.; Lodge, T. P.; Hanley, B.; Tirrell, M. *Macromolecules* **1987**, *20*, 1120.
(12) Sun, Z.; Wang, C. H. *Macromolecules* **1996**, *29*, 2011.
(13) Khatri, C. A.; Vaidya, M. M.; Levon, K.; Jha, S. K.; Green, M. M. *Macromolecules* **1995**, *28*, 4719.
(14) Canter, A. S.; Pecora, R. *Macromolecules* **1994**, *27*, 6817.
(15) Muthukumar, M.; Edwards, S. F. *Macromolecules* **1983**, *16*, 1475.
(16) Sato, T.; Teramoto, A. *Adv. Polym. Sci.* **1996**, *126*, 85.
(17) Ohshima, A.; Yamagata, A.; Sato, T.; Teramoto, A. *Macromolecules* **1999**, *32*, 8645.
(18) Murakami, H.; Norisuye, T.; Fujita, H. *Macromolecules* **1980**, *13*, 345.

(19) A dynamical mean-field theory of the dynamic structure factor for binary solutions of stiff polymers, presented previously,[17] can be extended to ternary solutions containing two stiff polymers. The result has the same form of the dynamic structure factor as that obtained by other workers[12,32,33] using different methods. This result predicted positive and negative c_P dependences of $(\Gamma/k^2)_{k=0}$ at low and high total polymer concentrations, respectively, which qualitatively agree with experimental results shown in Figure 4. However, the dependences were much weaker than the experiment, maybe owing to the neglect of internal motions of stiff polymers in the theory.
(20) Sato, T.; Ohshima, A.; Teramoto, A. *Macromolecules* **1998**, *31*, 3094.
(21) Jinbo, Y.; Sato, T.; Teramoto, A. *Macromolecules* **1994**, *27*, 6080.
(22) Yamakawa, H.; Fujii, M. *Macromolecules* **1974**, *7*, 128.
(23) Yamakawa, H.; Yoshizaki, T. *Macromolecules* **1980**, *13*, 633.
(24) Yamakawa, H. *Helical Wormlike Chains in Polymer Solutions*; Springer-Verlag: Berlin, 1997.
(25) Itou, T.; Chikiri, H.; Teramoto, A.; Aharoni, S. M. *Polym. J.* **1988**, *20*, 143.
(26) Itou, T.; Sato, T.; Teramoto, A.; Aharoni, S. M. *Polym. J.* **1988**, *20*, 1049.
(27) Sato, T.; Ohshima, A.; Teramoto, A. *Macromolecules* **1994**, *27*, 1477.
(28) Teraoka, I. Ph.D. Thesis, University of Tokyo, 1988.
(29) Fujiyama, T.; Sato, T.; Teramoto, A. *Acta Polym.* **1995**, *46*, 445.
(30) Hamada, M.; Sato, T.; Teramoto, A. Manuscript in preparation.
(31) Kasabo, F.; Kanematsu, T.; Nakagawa, T.; Sato, T.; Teramoto, A. *Macromolecules* **2000**, *33*, 2748.
(32) Benmouna, M.; Benoit, H.; Duval, M.; Akcasu, Z. *Macromolecules* **1987**, *20*, 1107.
(33) Foley, G.; Cohen, C. *Macromolecules* **1987**, *20*, 1891.
(34) Norisuye, T.; Tsuboi, A.; Teramoto, A. *Polym. J.* **1996**, *28*, 357.

MA000915Y